# scientific reports

OPEN

# Detection of $NO_3^-$ introduced in plasma-irradiated dry lettuce seeds using liquid chromatography-electrospray ionization quantum mass spectrometry (LC-ESI QMS)

Takamasa Okumura[1]✉, Pankaj Attri[2], Kunihiro Kamataki[1], Naoto Yamashita[1], Yuichi Tsukada[2], Naho Itagaki[1], Masaharu Shiratani[1], Yushi Ishibashi[3], Kazuyuki Kuchitsu[4] & Kazunori Koga[1,5]

Discharge plasma irradiates seeds with reactive oxygen and nitrogen species (RONS). However, RONS introduced in seeds by plasma irradiation have not been successfully detected thus far. This study provides experimental evidence that nitrate ion $NO_3^-$ is introduced in lettuce seeds as RONS upon irradiation with atmospheric-pressure air dielectric barrier discharge plasma. Plasma irradiation for 5 min promotes seed germination. The components of the plasma-irradiated seeds were examined using electrospray ionization quantum mass spectrometry (ESI QMS), which revealed that the plasma irradiation introduced an ion with a mass of 62 m/z in detectable amounts. This ion was identified as $NO_3^-$ by liquid chromatography (LC), multiple wavelength detector (MWD), and LC-ESI QMS. A one-dimensional simulation at electron temperature $T_e = 1$ eV, electron density $N_e = 10^{13}/m^3$, and gas temperature $T_g = 300$ K indicated the introduction of $NO_3^-$, involving nitric oxide NO. $NO_3^-$ is one of the most important ions that trigger signal transduction for germination when introduced in seeds. The scanning electron microscopy (SEM) images revealed that there was no change on the surface of the seeds after plasma irradiation. Plasma irradiation is an effective method of introducing $NO_3^-$ in seeds in a dry process without causing damage.

The growth improvement effect of plasma irradiation on plants has attracted considerable global attention[1–3]. Thus far, there have been pioneering studies on the improvement of germination and growth[4–19], control of hormone balance between gibberellic acid (GA) and abscisic acid (ABA) in seeds[20,21], and improvement of harvest characteristics[22] using plasma irradiation. Recently, molecular biological studies were conducted to elucidate the mechanisms underlying the biological effects of plasma irradiation[23]. Plasma can irradiate seeds with reactive oxygen and nitrogen species (RONS), photons, ions, and subjects them to electric fields[24]. RONS are involved in a variety of seed processes, including maturation, aging, and germination, followed by seedling growth[25,26]. Exogenous reactive oxygen species (ROS) improves *Zea mays* and *Helianthus annuus* seed germination by inducing GA biosynthesis and ABA catabolism[27]. Colorimetric determination and simulations are useful for estimating the amount of RONS introduced in seeds. However, RONS introduced in seeds by plasma irradiation have not been successfully detected thus far. Considering that many studies deal with the induction of biological responses in seeds upon plasma irradiation, discussions on their underlying mechanisms should

[1]Faculty of Information Science and Electrical Engineering, Kyushu University, Fukuoka 819-0395, Japan. [2]Center of Plasma Nano-Interface Engineering, Kyushu University, Fukuoka 819-0395, Japan. [3]Faculty of Agriculture, Kyushu University, Fukuoka 819-0395, Japan. [4]Faculty of Science and Technology, Department of Applied Biological Science, Tokyo University of Science, Chiba 278-8510, Japan. [5]Center for Novel Science Initiatives, National Institutes of Natural Sciences, Tokyo 105-0001, Japan. ✉email: t.okumura@plasma.ed.kyushu-u.ac.jp
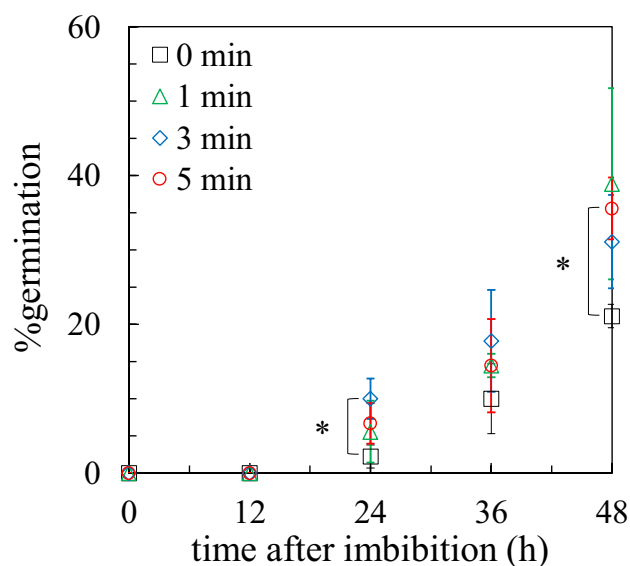
**Figure 1.** Germination characteristics of lettuce seeds without and with (1, 3, and 5)-min plasma irradiation.

be based on the actual particles introduced in the seeds. This study provides experimental evidence that nitrate ions $NO_3^-$ are introduced in seeds as RONS upon plasma irradiation.

We attempted to detect the typical RONS, $NO_3^-$, introduced in seeds upon irradiation with atmospheric-pressure air non-thermal plasma. Seed response to exogenous $NO_3^-$ administration is an important research subject in plant molecular physiology. $NO_3^-$ in plant seeds is responsible for inducing responses such as dormancy break, gene expression regulation, signal transduction, and ABA metabolism resulting from NLP8 binding to the *CYP707A2* promoter[28–32]. Although there are many studies on the changes in genotype and phenotype due to the administration of $NO_3^-$, the molecular mechanism behind the plant's response to $NO_3^-$ remains unclear[30]. Consequently, this study aimed to experimentally prove that $NO_3^-$ is introduced in seeds by plasma irradiation; a probable mechanism for this introduction is also suggested. It also proposed a new method of administering $NO_3^-$ to seeds in a dry process using plasma.

## Result and discussion

**Germination characteristics.** Considering that the introduction of $NO_3^-$ in seeds by plasma irradiation could raise the level of food production, lettuce (*Lactuca sativa* L.), which is the most commonly grown factory-plant[33], was used as biological material in anticipation of the rapid social implementation of plasma technology. Figure 1 shows the germination characteristics of seeds irradiated with plasma for 1, 3, and 5 min and non-irradiated seeds. This result was obtained using three biological replicates. The marks and error bars indicate average values and standard deviations, respectively. After 24 h, the seeds started to germinate with a relatively large deviation; the %germination was always higher in the seeds with (w/) plasma irradiation than in those without (w/o) plasma irradiation, suggesting that plasma irradiation promotes seed germination. This variability was probably due to the survival strategy of the plant and the amount of RONS introduced by the plasma. As the seed with 5 min of plasma irradiation had a 69% increase in its *p*-value compared to that (0.027) of the seed without plasma irradiation after 48 h upon two-tailed test, a plasma irradiation period of 5 min was decided for further experiments.

**Detection of plasma-induced unknown molecules in seeds.** Electrospray ionization quantum mass spectrometry (ESI QMS) was used to detect $NO_3^-$ in the seeds. Figure 2 shows the MS spectra of (a) ultra-pure water (blank), (b) the sample without plasma, and (c) the sample with 5 min plasma irradiation. Peaks $S_1$, $S_2$, $S_3$, $S_4$, $S_5$, and $S_6$ are shown in Fig. 2a–c. These peaks are observed even in ultra-pure water (Fig. 2a) and are thus assumed to have originated from the LC-QMS system. The intensities of peaks $S_1$ to $S_6$ in Fig. 1b and c are larger than those in Fig. 2a. This might be due to the matrix effect of seed contaminants. Conversely, the $M_1$ and $M_2$ peaks are found only for the seed extract in Fig. 1b and c, indicating that these two peaks originate from the seed material. The intensities of the $M_1$ and $M_2$ peaks in Fig. 2b are almost the same as those in Fig. 2c, indicating that the concentrations of the sample w/o and w/ plasma are the same and that plasma irradiation does not change the substantial composition in the mass range of 50–80 m/z. Nevertheless, a peak X at 62 m/z (indicated with an arrow) is clearly observed in Fig. 2c.

Further experiments were conducted to evaluate the reproducibility with five biological replicates. The MS spectra in the 60–64 m/z mass region of 20 seeds w/o plasma irradiation are shown in Fig. 3a, and those w/ plasma irradiation are shown in Fig. 3b. We performed three measurements per replicate and obtained the integrated values. The marks and error bars indicate average values and standard deviations, respectively. The relative intensity at 62 m/z without plasma irradiation was $131.96 \pm 0.31$, which was almost the same as the
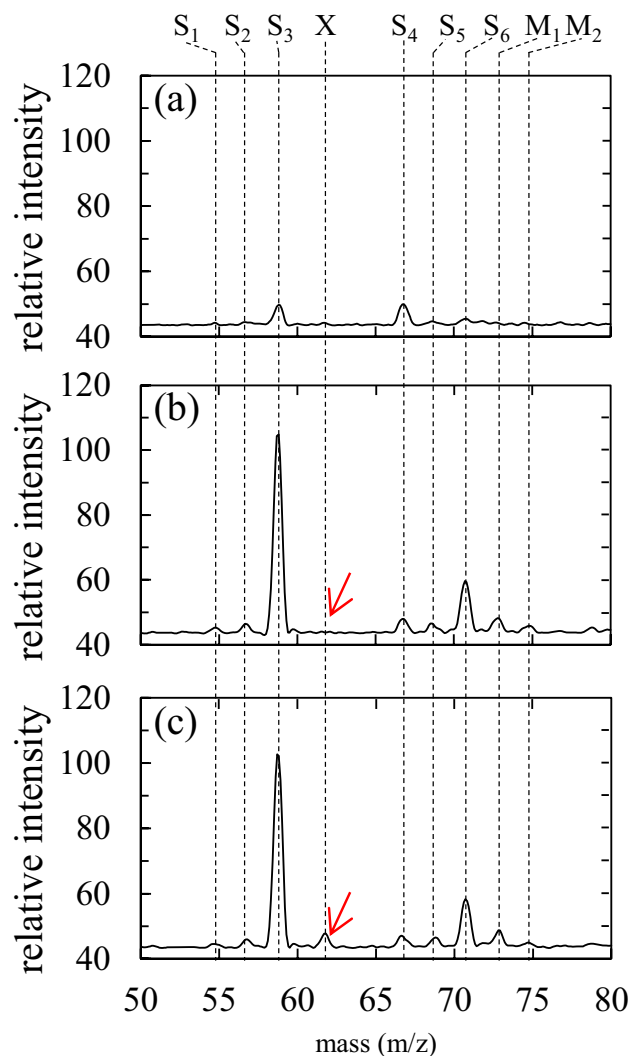
**Figure 2.** Typical MS spectra of (**a**) blank, and extract of 20 seeds (**b**) without plasma irradiation and (**c**) with 5 min plasma irradiation, obtained by QMS.

baseline (131) but was $141.53 \pm 1.83$ for seeds with plasma irradiation. The peak area was significantly higher in the extract w/ plasma ($p = 0.00012$ as determined by a two-tailed $t$-test) than in the extract w/o plasma irradiation. These results strongly indicate that 62 m/z molecules generated by plasma irradiation were introduced in the seeds. Considering that the optical emission spectra of scalable dielectric barrier discharge (SDBD) plasma show NO (200–250 nm)[34], a major candidate for peak X is nitrate ion ($NO_3^-$) among the long-lifetime species in air plasmas. $NO_3^-$ can be generated from the electron impact ionization reactions of $N_2$, $O_2$, and $H_2O$ in the gas phase as shown in the reactions (R1)–(R7)[35]
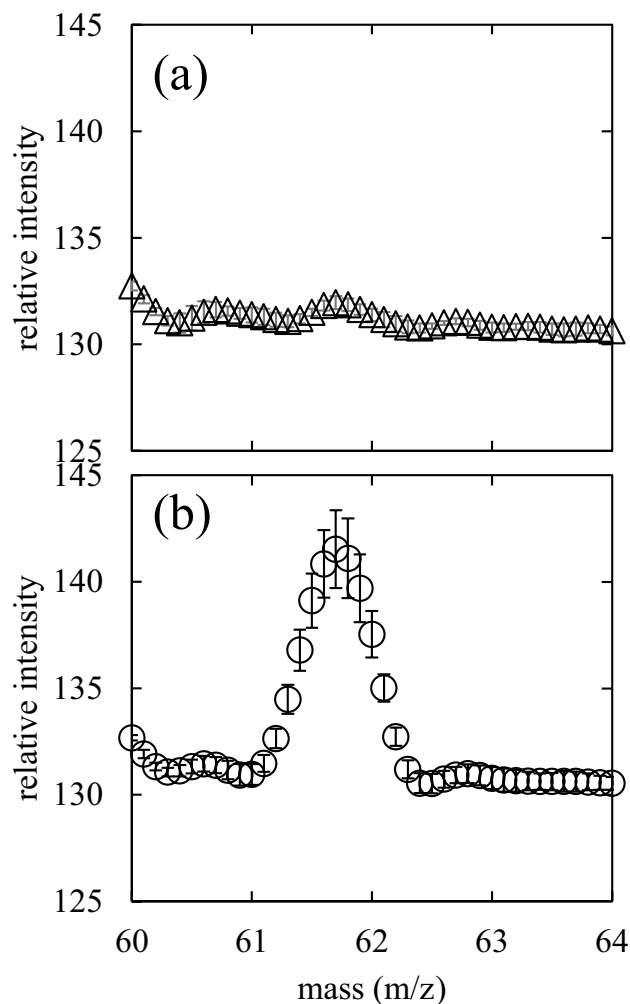
$$e + N_2 \rightarrow e + 2N \tag{R1}$$

$$e + H_2O \rightarrow e + H + OH \tag{R2}$$

$$e + O_2 \rightarrow 2O + e \tag{R3}$$

$$N + OH \rightarrow NO + H \tag{R4}$$

$$NO + O \rightarrow NO_2 \tag{R5}$$

$$NO_2 + e \rightarrow NO_2^- \tag{R6}$$

$$NO_2 + NO_2^- \rightarrow NO_3^- + NO \tag{R7}$$

**Figure 3.** MS spectrum of 60–64 m/z of extract of 20 seeds (**a**) without plasma irradiation and (**b**) with 5 min plasma irradiation, obtained by QMS mode. Three shots were integrated. Marks and error bars show mean values and standard deviations of triplicate, respectively.

**Identification of ion 62 m/z.**    A liquid chromatography (LC)-multiple wavelength detector (MWD) and LC-ESI QMS were used to identify the 62 m/z peak. Chromatography is effective in measuring the amount of $NO_3^-$ in seed extract from impurities such as enzymes, proteins, and organic metals therein. The nitrate ion absorbs a wavelength of ~ 224 nm, and its isosbestic point is 215 nm[36]. A wavelength of 210 nm was used for MWD to avoid interference by peptide bonds of protein, which absorb at 228 nm, in seed extract[37]. It has been reported that $NO_3^-$ is a major ion found in plasma-irradiated water[1,38]; hence, ultra-pure water was also irradiated with plasma and used for the analysis. Figure 4 shows the MWD chromatogram at 210 nm for (a) blank (ultra-pure water), (b) standard solution of $NO_3^-$ at 1 μM, (c) ultra-pure water without plasma irradiation, (d) ultra-pure water with plasma irradiation, (e) seed extract without plasma irradiation, and (f) seed extract with plasma irradiation. The disturbance observed within 2 min is due to the injection shock and is thus neglected. Figure 4a shows no peaks after 2 min in the blank (ultra-pure water used for preparing the seed extraction). Ultra-pure water was used to dilute the standard reagent $NO_3^-$. A peak corresponding to $NO_3^-$ appears at 5.84 min in the MWD, as shown in Fig. 4b. Although there is no $NO_3^-$ peak in Fig. 4c, we can find a peak with high intensity in Fig. 4d and f, showing that $NO_3^-$ is introduced in ultra-pure water and seeds by plasma irradiation. A small $NO_3^-$ peak was also observed in seeds without plasma irradiation. The seed extract had several peaks at 3–5 min, as shown in Fig. 4e and f, and the areas of these peaks are almost the same, whereas the $NO_3^-$ peak areas are significantly different from each other, i.e., 81.05 and 1486.04 for w/o and w/plasma, respectively. According to the Lambert–Beer law, the amount of $NO_3^-$ seems to be considerably high in the extracts of seeds subjected to plasma irradiation. However, it cannot be denied that plasma irradiation may have produced an ion in the seed, which may have absorbed UV at approximately 210 nm with the same retention time as that of $NO_3^-$. Therefore, we performed an LC-ESI QMS experiment, corresponding to the results of Figs. 2, 3, and 4.

The isotope distribution of a molecule to be analyzed is unique to its structure and very effective in identifying those that indicate the detected mass. As stable isotopes are present in each of the nitrogen and oxygen atoms, the
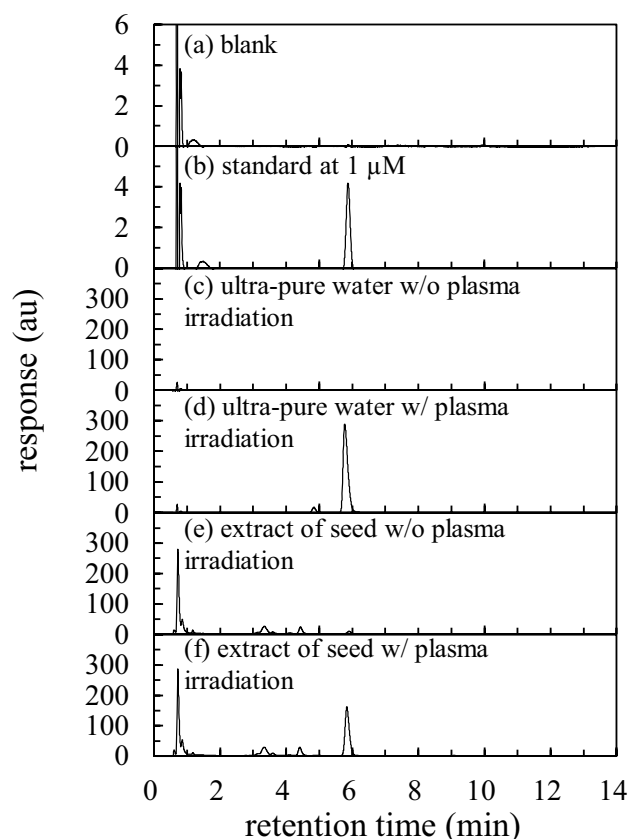
**Figure 4.** MWD chromatograms of 210 nm of (**a**) blank, (**b**) standard solution of $NO_3^-$ at 1 µM of concentration, ultra-pure water (**c**) without plasma irradiation and (**d**) with plasma irradiation for 300 s, and extract of seed (**e**) without plasma irradiation and (**f**) with plasma irradiation for 5 min.

proportion of $NO_3^-$ was calculated using the isotope distribution calculator (Agilent MassHunter Workstation Data Analysis Core; Version 10.0); using this we can estimate the mass that is dominantly detected for $NO_3^-$. The calculated values were 61.99 m/z, 62.99 m/z, 63.99 m/z, and 64.99 m/z of mass corresponding to 98.91%, 0.47%, 0.61%, and 0.00% of abundance, respectively, indicating that approximately 99% of $NO_3^-$ existing in nature gives a mass of 62 m/z. Consequently, to identify 62 m/z of $NO_3^-$, a chromatogram of 62 m/z was obtained for the standard reagent of $NO_3^-$ and extract of plasma-irradiated seeds. The mass resolution of the QMS was within 1 m/z. The coincidence of these retention times strongly indicated that they were the same substances. Although the signal intensity saturates at high concentrations for the extracted ion chromatogram (EIC), it can detect substances in smaller amounts compared to that by MWD. Figure 5 shows the ESI of 62 m/z for (a) blank, (b) standard solution of $NO_3^-$ at 1 µM, (c) ultrapure water without plasma irradiation, (d) ultrapure water with plasma irradiation, (e) seed extract without plasma irradiation, and (f) seed extract with plasma irradiation. Figure 5 was obtained from the same sample shown in Fig. 4 to eliminate the contamination and concentration variation within the dilution processes. There is no peak in the blank, as shown in Figs. 5a and 4a. The standard reagent showed a peak at 5.8–6.3 min retention time, as shown in Fig. 5b. Figure 5c and d show ultra-pure water with and without plasma, respectively. During the plasma irradiation, ultrapure water was placed in a quartz Petri dish. A peak does not appear in the ultra-pure water simply placed in the quartz Petri dish (without irradiation), as shown in Fig. 5c, whereas a large peak appears at 5.8–7.0 min retention time when the same sample is irradiated with plasma, as shown in Fig. 5d. This retention time was in the same range as that of the standard reagent. Thus, the 62 m/z ion obtained from plasma irradiation was identified as $NO_3^-$. For the seed extract, peaks were found in the same retention time region as that shown in Fig. 5e and f, suggesting that $NO_3^-$ was already present in the seed prior to plasma irradiation; its amount increased upon plasma irradiation. The standard deviations (±) in the mean peak areas for the seed extract were $4.6 \times 10^3 \pm 660.5$ and $3.9 \times 10^4 \pm 4154.9$ with and without plasma irradiation, respectively. The statistical $t$-test showed that $p = 0.0006$. Although it is clear that $NO_3^-$ was introduced in the seeds by plasma irradiation, it is also interesting that $NO_3^-$ was already present in the seeds at detectable levels prior to plasma irradiation. This method may be useful for measuring the amount of $NO_3^-$ originally present in untreated seeds.

**Introduction pathway of $NO_3^-$ into seeds by plasma irradiation.** The feasibility of $NO_3^-$ introduction in seeds by air SDBD plasma irradiation at atmospheric pressure was assessed by 1D simulation using COMSOL with 624 generation and decomposition reaction equations, summarized by Sakiyama et al.[39], wherein
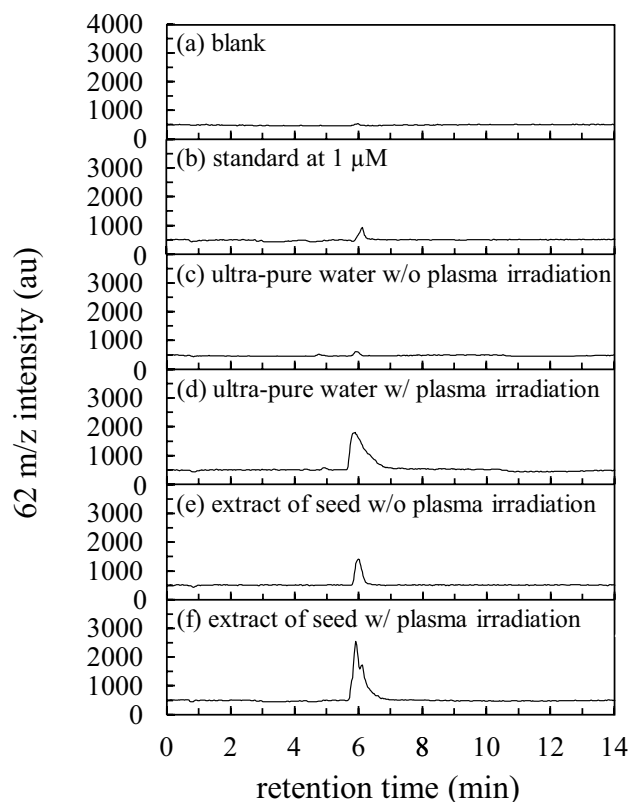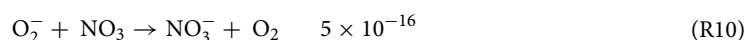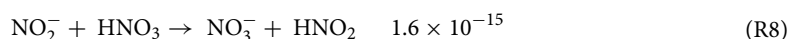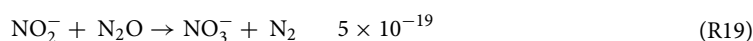
**Figure 5.** EIC of 62 m/z of (**a**) blank, (**b**) standard solution of $NO_3^-$ at 1 μM of concentration, ultra-pure wate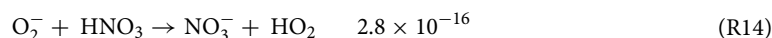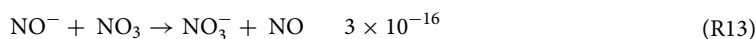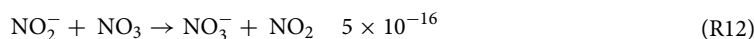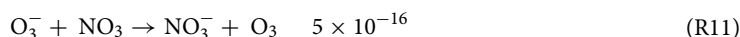r (**c**) without plasma irradiation and (**d**) with plasma irradiation for 5 min, and extract of seed (**e**) without plasma irradiation and (**f**) with plasma irradiation for 5 min.

| Chemical formula | Density (/m³) |
|---|---|
| $NO_3^-$ | $3.9 \times 10^3$ |
| NO | $6.6 \times 10^{18}$ |
| $NO_2$ | $1.4 \times 10^{10}$ |
| $NO_2^-$ | $1.1 \times 10^2$ |
| $NO_3$ | $1.0 \times 10^2$ |
| $HNO_3$ | $1.2 \times 10^{-1}$ |
| $HNO_2$ | $2.4 \times 10^{-10}$ |
| $N_2O_5$ | $2.2 \times 10^{-29}$ |

**Table 1.** 1D simulation result for density of $NO_x^-$ relating reactive species at a certain point such as seeds after 1000 s.

the electron temperature Te = 1 eV, electron density Ne = $10^{13}$/m³, gas temperature Tg = 300 K, and plasma width Lp = 0.1 mm for a time duration of 1000 s. The simulation results present the density of $NO_3^-$ and that of the reactive species involved in its generation at a point 5 mm away from the plasma region corresponding to the seed position. Table 1 shows the simulation results of the density at a certain point, e.g., seeds placed under the SDBD electrode after 1000 s, for $NO_3^-$ and the reactive species that participate in its generation through the following reactions[39–42]:

$$NO_2^- + HNO_3 \rightarrow NO_3^- + HNO_2 \quad 1.6 \times 10^{-15} \tag{R8}$$

$$NO_2^- + N_2O_5 \rightarrow NO_3^- + NO_3 + NO \quad 7 \times 10^{-16} \tag{R9}$$

$$O_2^- + NO_3 \rightarrow NO_3^- + O_2 \quad 5 \times 10^{-16} \tag{R10}$$

$$O_3^- + NO_3 \rightarrow NO_3^- + O_3 \quad 5 \times 10^{-16} \tag{R11}$$

$$NO_2^- + NO_3 \rightarrow NO_3^- + NO_2 \quad 5 \times 10^{-16} \tag{R12}$$

$$NO^- + NO_3 \rightarrow NO_3^- + NO \quad 3 \times 10^{-16} \tag{R13}$$

$$O_2^- + HNO_3 \rightarrow NO_3^- + HO_2 \quad 2.8 \times 10^{-16} \tag{R14}$$

$$O_3^- + NO_2 \rightarrow NO_3^- + O_2 \quad 2 \times 10^{-17} \tag{R15}$$

$$NO_2^- + O_3 \rightarrow NO_3^- + O_2 \quad 1.8 \times 10^{-17} \tag{R16}$$

$$O_3^- + NO \rightarrow NO_3^- + O \quad 1 \times 10^{-17} \tag{R17}$$

$$NO_2^- + NO_2 \rightarrow NO_3^- + NO \quad 4 \times 10^{-18} \tag{R18}$$

$$NO_2^- + N_2O \rightarrow NO_3^- + N_2 \quad 5 \times 10^{-19} \tag{R19}$$
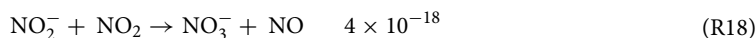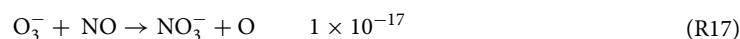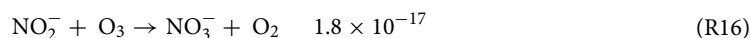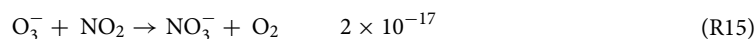
The unit of the rate constant corresponding to the aforementioned reactions is (m$^3$/s). Table 1 shows that $NO_3^-$ is directly transported to seeds along with the simultaneous transportation of the reactive species participating in its generation, such as NO, $NO_2$, $NO_2^-$, $NO_3$, $HNO_3$, $HNO_2$, and $N_2O_5$. The DBD plasma is accompanied by a streamer discharge. The reduced electric field E/N in the initial DBD plasma is approximately 100 Td and that in the typical streamer channel is < 30 Td[43]. In this state, the electron temperature $T_e$ < 2.7 eV, and such electrons are mainly consumed for the vibration excitation of $N_2$ and $O_2$ in the air at atmospheric pressure. The vibrational states of $N_2$ and $O_2$ contribute to the formation of NO through the following reactions, commonly known as the Zeldovich mechanism[44]. The activation energy $E_a$ and enthalpy of reaction $\Delta H$ both are nearly 3 eV/mol for R20, and 0.3 eV/mol and − 1 eV/mol for R21, respectively.

$$O\,(^3P) + N_2 *(^1\Sigma_g^+, v) \rightarrow NO(^2\Pi) + N(^4S), \tag{R20}$$

$$N + O_2 \rightarrow NO + O \tag{R21}$$
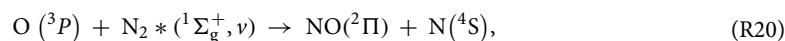
Hence, NO shows the highest density ($6.6 \times 10^{18}$/m$^3$) in Table 1. High-density NO may react with the $H_2O$ in the seeds. According to Lukes et al., NO leads to $NO_3^-$ through the following reaction[45].
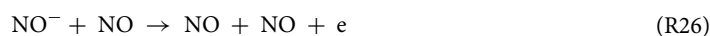
$$2NO + O_2 + H_2O \rightarrow 2H^+ + NO_2^- + NO_3^- \tag{R22}$$
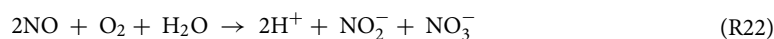
The lettuce seeds used in this study had an average weight ± standard deviation of approximately 0.8 ± 0.04 mg/seed (n = 8). Water content in more than 1250 seeds was measured and found to be 4.705 ± 0.503 wt% (n = 4). Using these mean values, the number of water molecules in the seed, $n_{H2O}$, was derived by Eq. (1):

$$n_{H2O} = \frac{wN_A}{M} \tag{1}$$

where $w$ is the weight of $H_2O$ in the seed (37.64 μg/seed), $N_A$ is the Avogadro constant ($6.022 \times 10^{23}$/mol), and $M$ is the $H_2O$ molar mass (18 g/mol). The seed area was $0.393 \pm 0.00374 \times 10^{-6}$ m$^2$ (n = 290), and the seed volume was derived to be $0.393 \times 10^{-9}$ m$^3$/seed, assuming a thickness of 1 mm. The volume of NO ($n_{NO}$) and $H_2O$ ($n_{H2O}$) in the seed were $2.594 \times 10^9$ and $1.259 \times 10^{18}$, respectively. When NO reacted with $H_2O$ in the seed, two molecules of NO and one molecule of $H_2O$ were consumed to bear $NO_2^-$ and $NO_3^-$, as shown in R22. Therefore, even if NO reacted completely with $H_2O$, sufficient $H_2O$ would remain in the seeds. Considering the high density of NO in a stable ($O_2$ and $H_2O$)-rich environment, it is concluded that the introduction pathway of $NO_3^-$ into seeds by plasma irradiation mainly involved reaction (R22). On the other hand, according to Sakiyama et al.[39], $NO_2^-$ reacts with NO and produces $NO^-$ and $NO_2$ by the following reaction[46].

$$NO_2^- + NO \rightarrow NO^- + NO_2 \tag{R23}$$

$NO^-$ reacts with M, $O_2$, and NO and produces NO, $O_2^-$, and e by the following reactions[47].

$$NO^- + M \rightarrow NO + M + e \tag{R24}$$

$$NO^- + O_2 \rightarrow NO + O_2^- \tag{R25}$$

$$NO^- + NO \rightarrow NO + NO + e \tag{R26}$$

NO is involved in R22. $O_2^-$ reacts with $N_2$ and $O_2$ and produces e by the following reactions[41].
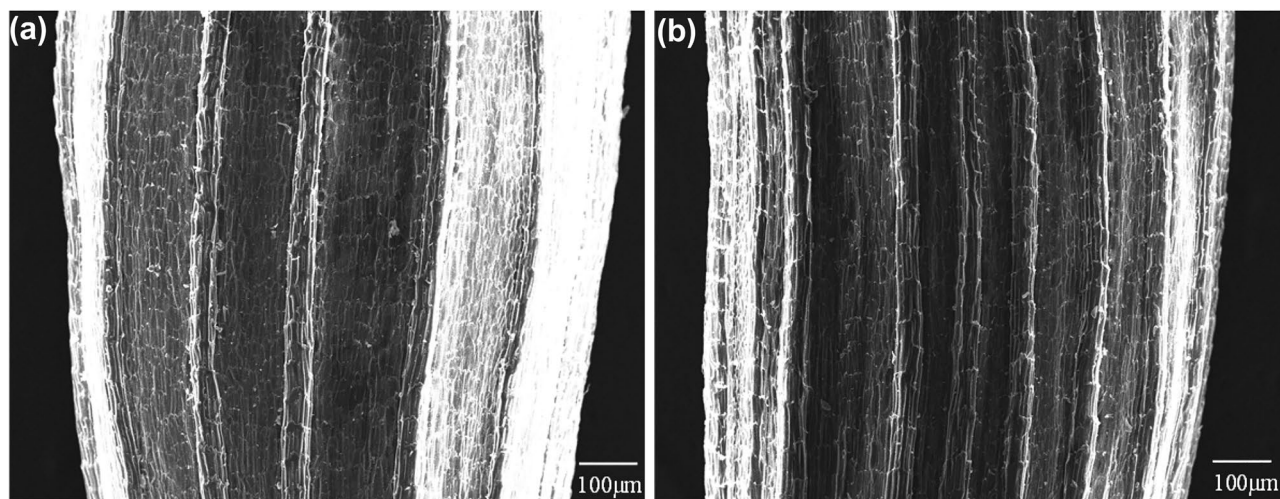
**Figure 6.** SEM image of the same seed (**a**) before plasma irradiation and (**b**) after plasma irradiation for 10 min.

$$O_2^- + N_2 \rightarrow N_2 + O_2 + e \qquad \text{(R27)}$$

$$O_2^- + O_2 \rightarrow O_2 + O_2 + e \qquad \text{(R28)}$$
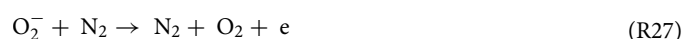
The electron e reacts with NO and $O_2$ and produces $NO^-$ and $O_2^-$ by the following reactions[39,41].

$$e + NO + M \rightarrow NO^- + M \qquad \text{(R29)}$$

$$e + O_2 \rightarrow O_2^- \qquad \text{(R30)}$$

$NO^-$ and $O_2^-$ are involved by reactions of R24-26 and R27, 28, respectively.

**Assessment of seed surface before and after plasma irradiation.** Figures 2 and 4 suggest that plasma irradiation did not affect the qualitative composition of the seeds. Therefore, the physical effects of plasma irradiation on the surface conditions of the seed coat were investigated using the scanning electron microscopy (SEM) images. Figure 6 shows a typical SEM image obtained (a) before and (b) after the plasma irradiation. The observed surface was the side on which the plasma was irradiated. The seeds were irradiated with plasma for 10 min, which was twice as long as the conditioning period of the seeds for mass spectroscopy. Lettuce seeds are composed of an outer layer, called the pericarp as the seed coat and integument, endosperm, and embryo as the internal organelle[48]. A typical pericarp was observed in the seeds used in this study, as shown in Fig. 6a. The pericarp remained intact after the plasma irradiation as shown in Fig. 6b. It is composed of a complex, dynamic extracellular matrix consisting of a network of carbohydrate polymers (cellulose, hemicellulose, and pectin) and structural proteins[48]. The chemical species produced by the plasma, such as $O_3$, may cleave or dimerize the carbon–carbon double bond (C=C) of alkene[49], including the unsaturated fatty acids in the lettuce seeds, followed by a C=C loss. Raman spectroscopy was used to assess such a chemical damage on the seed by plasma irradiation. A typical Raman spectrum at 980–1970 cm$^{-1}$ of lettuce seeds w/o plasma is shown in Fig. S1. We can find a peak at 1609 cm$^{-1}$, corresponding to C=C peak that is assigned to lignin and flavonoid (Fig. S1).

Raman spectroscopy revealed that the carbon–carbon double bond (C=C) peak assigned to lignin and flavonoid did not change after plasma irradiation for 5 and 10 min (Fig. S2). The chemical species produced by the plasma, such as $O_3$, may cleave or dimerize C=C of alkene[49], including the unsaturated fatty acids in the lettuce seeds, followed by a C=C loss, but such an effect is undetectable. These results suggest that plasma irradiation can introduce $NO_3^-$ without chemical or physical damage to the seeds.

## Conclusion

In this study, we developed a method for detecting $NO_3^-$ introduced in dry lettuce seeds by plasma irradiation using LC-ESI QMS. To date, only the amount of RONS in the gas phase and solution has been evaluated; this is the first time that plasma-introduced RONS in the treated seeds has been detected. As the molecular mechanism of the seed's cell response to $NO_3^-$ exogenously introduced in it is still under investigation, $NO_3^-$ remains one of the most important molecules in terms of seed physiology[30]. Thus far, the only method of exogenous administration of $NO_3^-$ in seeds has been to immerse them in a $KNO_3$ solution. However, plasma allows us to introduce $NO_3^-$ without the requirement of water or counterions. The quantitative evaluation of the amount of $NO_3^-$ introduced in seeds by plasma irradiation is decisive in the contribution of plasma science to plant molecular biology and the quantitative discussion of the germination induction mechanism by plasma irradiation.

## Methods

**Seed treatment and germination test.** Lettuce seed (*Lactuca sativa* L.) was purchased from Asahi Farm, Japan. The experimental use of plant materials was performed with the permission of Asahi Farm. The seeds were irradiated with plasma using a scalable dielectric discharge (SDBD) electrode[21]. The characteristics of the plasma used in this study have been discussed in a previous paper[9]. The plasma irradiation was performed at 24 °C using 55% Rh. For $NO_3^-$ detection, 80 lettuce seeds were irradiated simultaneously under a single plasma exposure. The irradiation time was determined to be 5 min based on the germination characteristics of seeds upon 0, 1, 3, and 5 min of plasma irradiation. The germination test was performed with 30 seeds sown on a paper filter in a petri dish, with 3 mL of tap water in a climate chamber at 22 °C under a light and dark cycle of 12 h each day. The number of germinated seeds was counted every 12 h after their imbibition for 48 h. The %germination was calculated by dividing the number of germinated seeds by the total number of seeds in the Petri dish. All methods were performed in accordance with the relevant guidelines and regulations.

**Sample preparation for mass spectrometry.** Twenty seeds were used to obtain a seed extract sample in the following procedure: The seeds were pulverized with beads in a 2.0 mL-tube (Eppendorf) using an automatic grinder at 2800 rpm for 3 min. Seed extraction was performed by shaking the pulverized sample with 50 µL of ultrapure water per mg of the sample at room temperature for 120 min under dark conditions. The seed extract was filtered using a membrane filter to remove the particles.

**Mass spectrometry.** We used ESI QMS (G6470A, Agilent) to detect $NO_3^-$ in the seeds, with a mobile phase of 3.75 mM ammonium acetate in 70% $H_2O$/30% acetonitrile. The mobile phase profile was 0.2 mL/min for ESI QMS and 0.4 mL/min for LC-ESI QMS. The injection volume was 5 µL. Ionization was performed in the negative mode of ESI with a 4000 V capillary voltage, 300 °C turbo gas temperature; and 50 V fragmentor voltage. Agilent Infinity II including LC (G7116A, Agilent) – MWD (G7165A, Agilent) were used for the identification and the quantitative analysis. Acclaim Trinity (P1, Thermo Fisher) was used as a column for LC. LC grade ultrapure water was used for the sample dilution. Standard reagent $NO_3^-$ was purchased from FUJIFILM Wako.

**1D simulation.** The 1D numerical model was developed using COMSOL Multiphysics 5.4, a multipurpose simulation software. Electrons exist in the plasma region at a constant number density of $10^{15}$ m$^{-3}$, as described in our earlier work[35]. We considered the particle distribution only in the x-direction (5 mm), normal to the surface of the seeds. We assumed $T_e = 1$ eV and $T_g = 300$ K. For the simulation, $H_2O$, $O_2$, and $N_2$ were in fractions of 0.01, 0.21, and 0.78, respectively. As mentioned in an earlier article, a coefficient value of $10^{-5}$ m²/s was used for this species[39]. The simulation was performed for 1000 s to determine the diffusion of the reactive species. All reaction pathways and rate constants were taken from the work of Sakiyama et al.[39].

**SEM.** Scanning electron microscopy (SEM) images were obtained using Hitachi S-3400 N, which has an emission current of 93 µA and acceleration voltage of 15 kV.

## Data availability

The datasets used and/or analysed during the current study available from the corresponding author on reasonable request.

## References

1. Attri, P., Ishikawa, K., Okumura, T., Koga, K. & Shiratani, M. Plasma agriculture from laboratory to farm: A review. *Processes* **8**, 1002 (2020).
2. Attri, P., Koga, K., Okumura, T. & Shiratani, M. Impact of atmospheric pressure plasma treated seeds on germination, morphology, gene expression and biochemical responses. *Jpn. J. Appl. Phys.* **60**, 1–7 (2021).
3. Attri, P. *et al.* Outcomes of pulsed electric fields and nonthermal plasma treatments on seed germination and protein functions. *Agronomy* **12**, 1–22 (2022).
4. Dobrin, D., Magureanu, M., Mandache, N. B. & Ionita, M. D. The effect of non-thermal plasma treatment on wheat germination and early growth. *Innov. Food Sci. Emerg. Technol.* **29**, 255–260 (2015).
5. Meng, Y. *et al.* Enhancement of germination and seedling growth of wheat seed using dielectric barrier discharge plasma with various gas sources. *Plasma Chem. Plasma Process.* **37**, 1105–1119 (2017).
6. Junior, C. A., De Oliveira Vitoriano, J., Da Silva, D. L. S., De Lima Farias, M. & De Lima Dantas, N. B. Water uptake mechanism and germination of *Erythrina velutina* seeds treated with atmospheric plasma. *Sci. Rep.* **6**, 1–7 (2016).
7. Da Silva, D. L. S., Farias, M. D. L., Vitoriano, J. D. O., Alves Júnior, C. & Torres, S. B. Use of atmospheric plasma in germination of *Hybanthus calceolaria* (L.) Schulze-Menz seeds. *Rev. Caatinga* **31**, 632–639 (2018).
8. Kitazaki, S., Sarinont, T., Koga, K., Hayashi, N. & Shiratani, M. Plasma induced long-term growth enhancement of *Raphanus sativus* L. using combinatorial atmospheric air dielectric barrier discharge plasmas. *Curr. Appl. Phys.* **14**, S149–S153 (2014).
9. Koga, K. *et al.* Simple method of improving harvest by nonthermal air plasma irradiation of seeds of *Arabidopsis thaliana* (L.). *Appl. Phys. Express* **9**, 5–8 (2016).
10. Koga, K. *et al.* Impact of radish sprouts seeds coat color on the electron paramagnetic resonance signals after plasma treatment. *Jpn. J. Appl. Phys.* **59**, 01 (2020).
11. Yawirach, S., Sarapirom, S. & Janpong, K. The effects of dielectric barrier discharge atmospheric air plasma treatment to germination and enhancement growth of sunflower seeds. *J. Phys. Conf. Ser.* **1380**, 012148 (2019).
12. Li, Y. *et al.* Air atmospheric dielectric barrier discharge plasma induced germination and growth enhancement of wheat seed. *Plasma Chem. Plasma Process.* **37**, 1621–1634 (2017).
13. Li, L. *et al.* Effects of cold plasma treatment on seed germination and seedling growth of soybean. *Sci. Rep.* **4**, 1–7 (2014).

14. Volkov, A. G., Hairston, J. S., Patel, D., Gott, R. P. & Xu, K. G. Cold plasma poration and corrugation of pumpkin seed coats. *Bioelectrochemistry* **128**, 175–185 (2019).
15. Molina, R. *et al.* Influence of irrigation conditions in the germination of plasma treated Nasturtium seeds. *Sci. Rep.* **8**, 1–11 (2018).
16. Pawlat, J. *et al.* Effects of atmospheric pressure plasma generated in GlidArc reactor on *Lavatera thuringiaca* L. seeds' germination. *Plasma Process. Polym.* **15**, 1700056 (2018).
17. Štěpánová, V. *et al.* Atmospheric pressure plasma treatment of agricultural seeds of cucumber (*Cucumis sativus* L.) and pepper (*Capsicum annuum* L.) with effect on reduction of diseases and germination improvement. *Plasma Process. Polym.* **15**, 1–9 (2018).
18. Tong, J. *et al.* Effects of atmospheric pressure air plasma pretreatment on the seed germination and early growth of andrographis paniculata. *Plasma Sci. Technol.* **16**, 260–266 (2014).
19. Fadhlalmawla, S. A., Mohamed, A. A. H., Almarashi, J. Q. M. & Boutraa, T. The impact of cold atmospheric pressure plasma jet on seed germination and seedlings growth of fenugreek (*Trigonella foenum-graecum*). *Plasma Sci. Technol.* **21**, 105503 (2019).
20. Mildažienė, V. *et al.* Treatment of common sunflower (*Helianthus annus* L.) seeds with radio-frequency electromagnetic field and cold plasma induces changes in seed phytohormone balance, seedling development and leaf protein expression. *Sci. Rep.* **9**, 1–12 (2019).
21. Attri, P. *et al.* Impact of seed color and storage time on the radish seed germination and sprout growth in plasma agriculture. *Sci. Rep.* **11**, 1–10 (2021).
22. Hashizume, H. *et al.* Improvement of yield and grain quality by periodic cold plasma treatment with rice plants in a paddy field. *Plasma Process. Polym.* **18**, 1–11 (2021).
23. Suriyasak, C. *et al.* Alterations of DNA methylation caused by cold plasma treatment restore delayed germination of heat-stressed rice (*Oryza sativa* L.) seeds. *ACS Agric. Sci. Technol.* **1**, 5–10 (2021).
24. Tochikubo, F. & Teich, T. H. Optical emission from a pulsed corona discharge and its associated reactions. *Jpn. J. Appl. Phys. Part 1* **39**, 1343–1350 (2000).
25. Bailly, C., El-Maarouf-Bouteau, H. & Corbineau, F. From intracellular signaling networks to cell death: The dual role of reactive oxygen species in seed physiology. *C. R. Biol.* **331**, 806–814 (2008).
26. Barba-Espín, G. *et al.* Understanding the role of H 2O 2 during pea seed germination: A combined proteomic and hormone profiling approach. *Plant Cell Environ.* **34**, 1907–1919 (2011).
27. Li, Z. *et al.* The synergistic priming effect of exogenous salicylic acid and H2O2 on chilling tolerance enhancement during maize (*Zea mays* L.) seed germination. *Front. Plant Sci.* **8**, 1–14 (2017).
28. Wang, R., Xing, X. & Crawford, N. Nitrite acts as a transcriptome signal at micromolar concentrations in arabidopsis roots. *Plant Physiol.* **145**, 1735–1745 (2007).
29. Matakiadis, T. *et al.* The *Arabidopsis abscisic* acid catabolic gene CYP707A2 plays a key role in nitrate control of seed dormancy. *Plant Physiol.* **149**, 949–960 (2009).
30. Yan, D. *et al.* NIN-like protein 8 is a master regulator of nitrate-promoted seed germination in Arabidopsis. *Nat. Commun.* **7**, 1–11 (2016).
31. Liu, K. H. *et al.* Discovery of nitrate-CPK-NLP signalling in central nutrient-growth networks. *Nature* **545**, 311–316 (2017).
32. Duermeyer, L. *et al.* Regulation of seed dormancy and germination by nitrate. *Seed Sci. Res.* **28**, 150–157 (2018).
33. Takeshima, H. & Joshi, P. K. Protected agriculture, precision agriculture, and vertical farming. *Int. Food Policy Res. Inst.* **49**, 1–10 (2019).
34. Attri, P. *et al.* Impact of Gamma rays and DBD plasma treatments on wastewater treatment. *Sci. Rep.* **8**, 1–11 (2018).
35. Attri, P., Koga, K., Okumura, T., Takeuchi, N. & Shiratani, M. Green route for ammonium nitrate synthesis: Fertilizer for plant growth enhancement. *RSC Adv.* **11**, 28521–28529 (2021).
36. Bolzan, R. M., Rafael, C., Giuseppe, L., Squadrito Rao, M. & Uppu William, A. P. Direct and simultaneous ultraviolet second-derivative spectrophotometric determination of nitrite and nitrate in preparations of peroxynitrite. *Methods Enzymol.* **301**, 178–187 (1999).
37. Koide, T., Ikenaka, T., Ikeda, K. & Hamaguchi, K. Studies on soybean trypsin inhibitors. *J. Biochem.* **75**, 805–823 (1974).
38. Judée, F., Simon, S., Bailly, C. & Dufour, T. Plasma-activation of tap water using DBD for agronomy applications: Identification and quantification of long lifetime chemical species and production/consumption mechanisms. *Water Res.* **133**, 47–59 (2018).
39. Sakiyama, Y., Graves, D. B., Chang, H. W., Shimizu, T. & Morfill, G. E. Plasma chemistry model of surface microdischarge in humid air and dynamics of reactive neutral species. *J. Phys. D. Appl. Phys.* **45**, 425201 (2012).
40. Dorai, R. & Kushner, M. J. A model for plasma modification of polypropylene using atmospheric pressure discharges. *J. Phys. D. Appl. Phys.* **36**, 666–685 (2003).
41. Capitelli, M. & Ferreira, C. M. *Plasma Kinetics in Atmospheric Gases* (Springer, 2001).
42. Fernandes, H. M. Monte Carlo simulations of two-dimensional hard core lattice gases. *Adv. Chem. Phys.* **42**, 1–610 (2007).
43. Komuro, A., Suzuki, K., Yoshida, K. & Ando, A. Characteristics of spatiotemporal variations of primary and secondary streamers under pulsed-voltage in air at atmospheric pressure. *Jpn. J. Appl. Phys.* **59**, 03 (2020).
44. Patil, B. S., Wang, Q., Hessel, V. & Lang, J. Plasma N2-fixation: 1900–2014. *Catal. Today* **256**, 49–66 (2015).
45. Lukes, P., Clupek, M., Babicky, V., Janda, V. & Sunka, P. Generation of ozone by pulsed corona discharge over water surface in hybrid gas-liquid electrical discharge reactor. *J. Phys. D. Appl. Phys.* **38**, 409–416 (2005).
46. Anicich, V. G. Evaluated bimolecular ion-molecule gas phase kinetics of positive ions for use in modeling planetary atmospheres, cometary comae, and interstellar clouds. *J. Phys. Chem. Ref. Data* **22**, 1469–1569 (1993).
47. Mcfarland, M., Dunkin, D. B., Fehsenfeld, F. C., Schmeltekopf, A. L. & Ferguson, E. E. Collisional detachment studies of NO⁻. *J. Chem. Phys.* **56**, 2358–2364 (1972).
48. Nijsse, J., Erbe, E., Brantjes, N. B. M., Schel, J. H. N. & Wergin, W. P. Low-temperature scanning electron microscopic observations on endosperm in imbibed and germinated lettuce seeds. *J. Chem. Phys.* **516**, 509–516 (1998).
49. Criegee, R. Mechanism of ozonolysis. *Angew. Chem. Int. Ed.* **14**, 745–752 (1975).

## Acknowledgements

## Author contributions

T.O. and K.Koga designed the study, prepared and characterized the samples, and wrote the manuscript. T.O. performed the experiments. T.O., K.Koga, A.P. and K.Kamataki discussed the chemical reaction simulations. T.O., K.Koga, Y.T., Y.I., and K.Kuchitsu discussed the biological significance of nitrate ion introduction. T.O., K.Koga, N.I., N.Y., and M.S. discussed the chemical reactions in gas phase. T.O., K.Koga, A.P., and M.S. discussed the organization of manuscript.

## Competing interests

The authors declare no competing interests.

## Additional information

**Supplementary Information** The online version contains supplementary material available at https://doi.org/10.1038/s41598-022-16641-1.

**Correspondence** and requests for materials should be addressed to T.O.

**Reprints and permissions information** is available at www.nature.com/reprints.

**Publisher's note**  Springer Nature remains neutral with regard to jurisdictional claims in published maps and institutional affiliations.